Effect of Single-Walled Carbon Nanotube on the Properties of Tetra Substituted Zinc Phthalocyanine-Uridine Conjugate

Racheal O. Awolope[1,*], Ikechukwu P. Ejidike[1,2], Tebello Nyokong[3]

[1]Department of Chemical Sciences, Faculty of Natural, Applied and Health Sciences, Anchor University, Lagos 100006, Nigeria
[2]Department of Chemistry, College of Science, Engineering, and Technology, University of South Africa, Florida 1709, South Africa
[3]Department of Chemistry, Rhodes University, Grahamstown 6140, South Africa

ABSTRACT

Combined-mediated therapy for cancer treatment is gaining urgent attention due to the overwhelming side effects of conventional chemotherapy. The use of single-walled carbon nanotubes (SWCNTs), as a drug delivery agent, will improve the selectivity, efficacy, and properties of tetra-substituted zinc phthalocyanine (ZnTPCPc) as a photodynamic agent during photodynamic therapy. The effect of SWCNT and uridine on the properties of ZnTPCPc was studied. Uridine was chemically linked to ZnTPCPc to form ZnTPCPc-uridine (2) which was further adsorbed onto SWCNT-COOH to give a combined photoactive complex represented as ZnTPCPc-uridine-SWCNT (3). Fluorescence and laser flash spectroscopy were used to determine the photophysical parameters, while thermogravimetric analysis (TGA), Raman spectroscopy, Transmission Electron Microscopy (TEM), UV-visible and Fourier transform infrared (FTIR) spectroscopy were used to characterize the complexes. Characteristics Q-band of metallated phthalocyanine was observed for the derivatives of ZnTPCPc, complexes 1, 2, and 3 exhibited Q-band maxima at 680 nm. Changes in the TGA pattern, TEM image, Raman peaks, and FTIR spectra show that complexes 2 and 3 were successfully formed. Despite the presence of SWCNT in ZnTPCPc-uridine-SWCNT, the fluorescence and triplet quantum yield increases; this indicates that the quenching effects of SWCNT were not observed in complex 3. The photophysical properties of the complexes, especially the high triplet quantum yield result suggest that the new combined photoactive complex could be a potential drug for the treatment of cancer.

Keywords: Fluorescence; Single-walled carbon nanotubes; Triplet quantum yields; Uridine; Zinc tetra-phenoxycarboxy phthalocyanine

1. Introduction

The biomedical application of single-walled carbon nanotubes (SWCNTs) has grown tremendously, due to their unique physicochemical properties, such as great strength, flexibility, molecule-adsorptive surface area, high impact ratio, and their photothermal effect (PTT) which makes SWCNTs a potential PTT agent in cancer therapy [1-3]. However, the challenges of uniform dispersion due to aggregation, and toxicity of pristine SWCNTs have limited their application in commercial scale. To overcome these limitations of SWCNTs, research work has shown that functionalization, for example, the introduction of carboxyl, amino groups, or conjugation to other compounds has greatly overridden the issues around its applicability in medicine [4-6]. In this work, the properties of SWCNTs were examined after adsorption through π-π interaction with the conjugate of zinc phthalocyanine-uridine (tetra-substituted).

Zinc phthalocyanine (ZnPc) is a photodynamic agent; the combination of ZnPc, the light of appropriate wavelength, and molecular oxygen leads to the generation of singlet oxygen, a reactive oxygen specie and cytotoxic agent resulting in the irreversible destruction of cancerous cells during photodynamic therapy [7-10]. ZnPcs are examples of metallophthalocyanines (MPcs) in different clinical trial stages [11]. To improve the efficiency, specificity, solubility, and selectivity of ZnPc to cancerous cells, its conjugation to biomolecules is being explored [12, 13]. Uridine is overexpressed in breast cancer [14] and it improved the photophysical and photodynamic properties of MPc after linkage [15-18]. The transportation of PDT agents to target cells could limit its application to different cancerous tissues or organs. Thus, the adsorption of ZnPc-conjugate to SWCNTs is a developing strategy to deliver the potential cancer drugs. SWCNTs have hollow and cage-like interiors through which they can anchor drugs [19-21]. Herein, we report for the first time the photophysical properties of conjugates of uridine with zinc tetra phenoxy carboxy phthalocyanine (ZnTPCPc) in the presence or absence of SWCNT.

2. Experimental
2.1 Materials

Single-walled carbon nanotubes (SWCNT-COOH, 1-5 nm in diameter and 1-5 μm in length) were obtained from Nanolab. Dimethylsulphoxide (DMSO) N, N'-Dicyclohexylcarbodiimide (DCC) and dimethylformamide (DMF), chloroform, hexane and tetrahydrofuran (THF), Zinc phthalocyanine (ZnPc), uridine, dimethylaminopyridine (DMAP), were obtained from SAARCHEM. ZnTPCPc (1) [22] was synthesized according to literature methods.

2.2 Equipment

Infrared spectra were recorded on a Perkin-Elmer Universal ATR Sampling accessory spectrum 100 FT-IR spectrometer. Transmission electron microscopy (TEM) images were obtained using a Zeiss Libra TEM 120 model operated at 90 kV. Mass spectra data were collected with a Bruker AutoFLEX III Smartbeam TOF/TOF mass spectrometer [23, 24]. Raman spectra were obtained with a Bruker Vertex 70 - Ram II spectrometer (equipped with a 1064 nm Nd: YAG laser and liquid nitrogen-cooled germanium detector), and solid samples diluted with KBr were used. Thermal gravimetric analysis (TGA) was recorded on a Shimadzu DTG-TG 60H with a gas flow of 120 ml/min and operated under a nitrogen atmosphere at 10 ºC /min.

Absorption spectra were recorded on a Shimadzu UV-Vis 2550 spectrophotometer and fluorescence emission and excitation spectra were examined on a Varian Eclipse spectrofluorimeter using a 360-1100 nm filter. Laser flash photolysis experiments were performed to determine the triplet decay kinetics [24]. Solutions for triplet state studies were de-aerated with argon for 15 min before measurement.

2.3 Synthesis

2.3.1 Synthesis ZnTPCPc-Uridine (2) conjugate, Fig. 1A

A mixture of ZnTPCPc (1) (0.2 g, 0.18 mmol) and DCC (0.06 g 0.29 mmol) in 4 ml of DMF was stirred for 2 h under argon at room temperature. Afterward, DMAP (0.01 g, 0.08 mmol) was added and the reaction mixture was stirred for 24 h. Uridine (0.16 g, 0.72 mmol) was added and the mixture was further stirred for 48 h. The reaction mixture was poured into 40 ml of distilled water and extracted with 40 ml of chloroform three times. The solid product (ZnTPCPc-uridine (2)) was purified by silica gel column chromatography using the solvent mixture of THF and hexane (95:5 v/v) as eluent, following a procedure reported by [25] with modification.

ZnTPCPc-uridine (2): Yield 64 % (0.09 g), UV–Vis (DMSO), λmax (nm) (log ε): 679 (5.3), 615 (4.2), 353 (4.8). Anal. Calc. for $C_{96}H_{84}N_{20}O_{28}Zn$: C, 56.77; H, 4.17; N, 13.79. Found: C, 57.38; H, 4.58; N, 14.86 %. MALDI-TOFMS (m/z): 2031 g/mol, Found: 2029. IR [(ATR) vmax/cm^{-1}]; 3402 - 3058 (OH str.), 1694 and 1597 (C=O), 1226 (OH bend), 1087 and 1043 (C-O-C).

2.3.2 Synthesis of ZnTPCPc-uridine-SWCNT (3), Fig. 1B

ZnTPCPc-uridine (2) was adsorbed on SWCNT-COOH according to literature methods for adsorbing of other Pc [26] with slight modification as follows: 20 mg of SWCNT-COOH were ultra-sonicated for 60 min in 3 ml of DMF to give a brown coloured suspension which was further centrifuged for 20 min at 3500 rpm to get rid of large bundles of SWCNT-COOH, the supernatant was used for experiments. ZnTPCPc-uridine (0.2 g, 0.098 mmol) was then added to the solution to give a blue suspension and the resulting mixture was stirred for 5 days to give a dark blue solution indicating the formation complex 3. The reaction mixture was poured into 20 ml of distilled water and was extracted using chloroform three times. The chloroform fraction was allowed to dry in a vacuum. The solid product was purified using size exclusion chromatography.

ZnTPCPc-uridine-SWCNT (3): UV–Vis λmax nm 680, IR [(ATR) vmax/cm^{-1}]; 3402 - 3169 (O-H str.), 1597 (C=O), 1233 (OH bend), 1143 and 1091 (C-O-C str.). [Raman vmax/cm^{-1}]: 2549 (G*), 1591 (G), 1278 (D).

2.3.3 Photophysical and photochemical parameters

Triplet $\left(\Phi_T\right)$ and fluorescence $\left(\Phi_F\right)$ quantum yields for complexes 2 and 3 were determined using the comparative methods as previously described [27-30]. ZnPc in DMSO was employed as a standard for triplet quantum yield ($\Phi_T = 0.65$ [28] and fluorescence quantum yield ($\Phi_F = 0.20$, [29]).

3. Results and Discussion

The synthetic route for the formation of ZnTPCPc-uridine (2) and ZnTPCPc-uridine-SWCNT (3) is shown in Fig 1. ZnTPCPc-uridine is an esterification reaction between ZnTPCPc and uridine, while ZnTPCPc-uridine-SWCNT was formed by adsorbing ZnTPCPc-uridine on SWCNT through a π-π interaction.

Fig. 1. Synthetic route for the formation of complex 2 and 3.
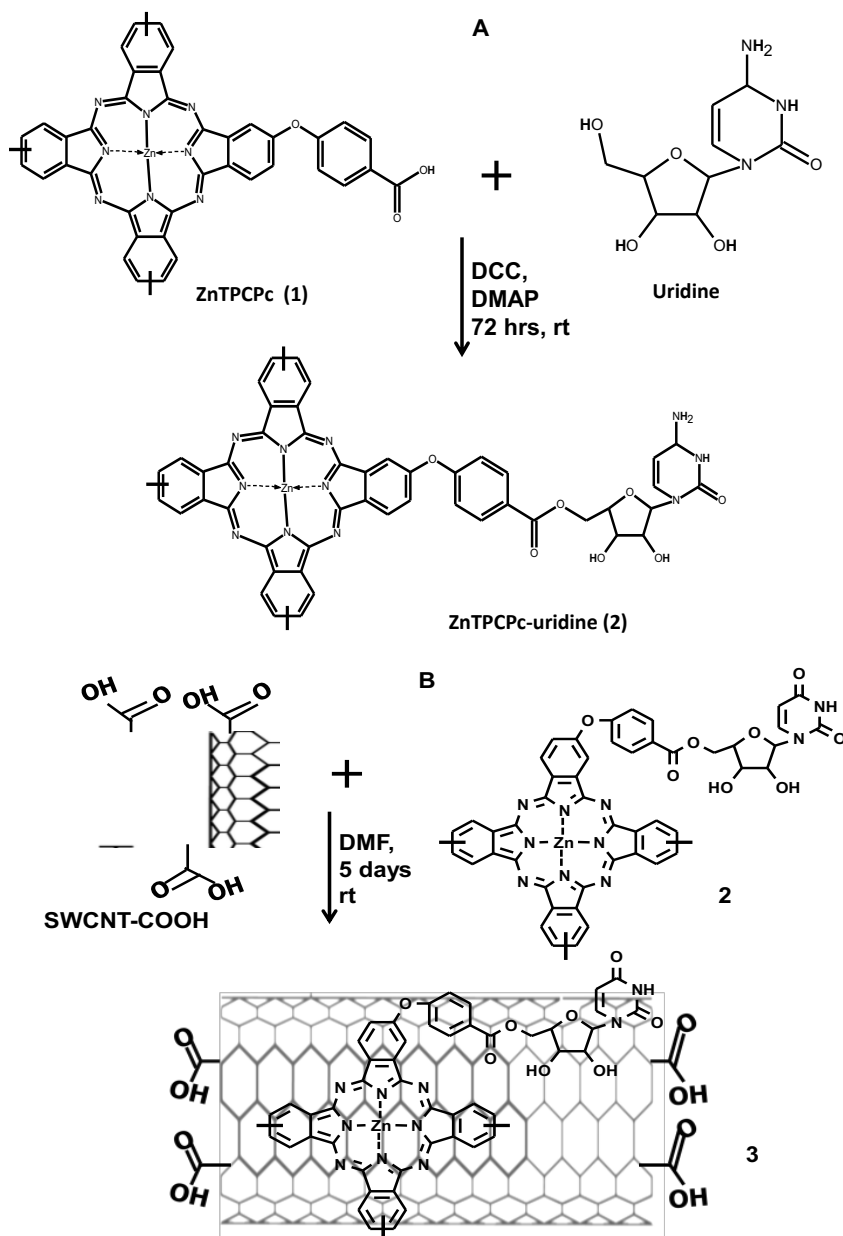
3.1 UV and FTIR Characterization of Complexes 2 and 3

Complexes 2 and 3 show three peaks at 347, 609, and 676 nm of a symmetrically substituted metallated phthalocyanine which is usually characterized by a single Q-band as shown in complexes 2 and 3 (Fig. 2), while un-metallated Pcs and unsymmetrically substituted MPcs might display split Q-band depending on the solvent. A single Q-band where observed for complexes 2 and 3, these peaks were the same for the compounds except for differences in peak intensity. The peaks are similar to what has been reported before for MPc which usually exhibits a prominent peak between 650 to 1000 nm depending on the substituents with a base peak around 610 nm, and a B-band between 300 - 400 nm [31, 32].

The FTIR data (Table 1) confirm the successful formation of ZnTPCPc-uridine (2) and ZnTPCPc-uridine-SWCNT (3). The (OH) str. of ZnTCPc shifted to a longer wavelength on the formation of ZnTPCPc-uridine; the bathochromic shift may be as a result of the presence of OH groups in uridine, and these may also account for other changes in the peaks observed for complex 2. The shift in peaks or appearance of new peaks for complexes 2 and 3 were quite different for either ZnTCPc or SWCNT-COOH alone indicating successful conjugation.

Table 1. FTIR data of complexes 1-3.

Compound	ZnTCPc	ZnTPCPc-Uridine (2)	ZnTPCPc-uridine-SWCNT (3)	SWCNT-COOH
v(OH)str.	3372 - 2840	3402 - 3058	3402 - 3169	3296 - 3200
v(C=O)	1711	1694, 1597	1597	1751
v(O-H)bend	1597, 11391	1226	1143	-
v(C-O-C)	1090	1087, 1043	1091	-
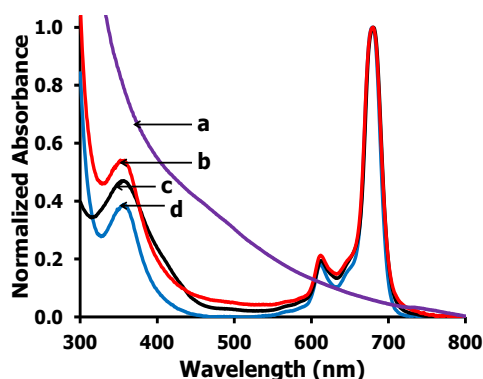
Fig. 2. Absorption spectra of SWCNT-COOH (a), ZnTPCPc-uridine-SWCNT, 3 (b), ZnTPCPc, 1 (c) and ZnTPCPc uridine, 2 (d).

3.2 Thermogravimetric analysis (TGA)

Thermogravimetric analysis (TGA) shows the weight loss (%) of a sample concerning an increase in temperature. As the temperature increases, the weight percentage decreases due to different reactions which correspond to changing mass. The TGA profiles of the complexes were obtained under a steady flow of N_2, at a heating rate of 10 °C min^{-1}. Fig. 3 shows different thermal decay profiles of complexes 3, SWCNT-COOH, and 2. The different thermal stability of the complexes as depicted by their percentage weight loss show that the complexes have different chemical and structural formulations.
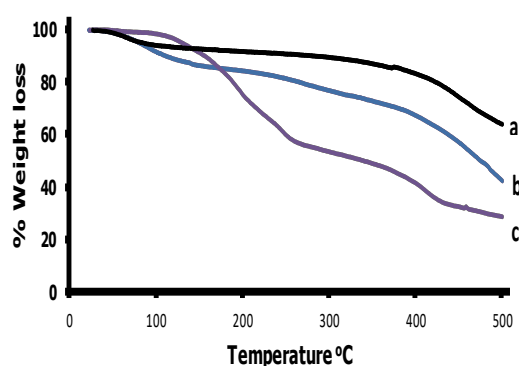
Fig. 3. The thermal decay profile of ZnTPCPc-uridine-SWCNT (3) (a), SWCNT-COOH (b), and ZnTPCPc-uridine (2) (c).

Complex 2 was less stable at high temperatures showing 28.5 % weight loss at 500 °C. At low temperatures, up to 150 °C, it showed only 91.5 % weight loss; however, as the temperature increases it steadily loses weight due to different functional groups such as -NH₂, -OH breaking off (Table 2). SWCNT-COOH was more stable than complex 2, showing 42.6 % weight loss at 500 °C. The thermal stability of ZnTPCPc-Uridine (2) improved on adsorption to SWCNT-COOH to form ZnTPCPc-Uridine-SWCNT (3) showing 64.1 % weight loss at 500 °C; this can be attributed to the thermal strength of SWCNT [33]. The initial mass loss experienced (at ~

100 °C), as shown in Table 2 for each sample, may be attributed to solvent losses such as H_2O which has a boiling point of 100 °C. Decomposition of functional groups (such as –COOH, -NH$_2$, -OH) and CH_2 found in SWCNT will occur between the temperature range of 100-250 °C [34, 35]. At about 350 °C ZnTPCPc-Uridine (2) experienced a 48.9 % weight loss as shown in Table 2 due to the breaking of the pyrrole units of the complex.

The increase in stability of ZnPc compounds used in this report on adsorption to SWCNT corresponds with the literature. Ogbodu et al. [12] reported an increase in ZnPc- spermine conjugate adsorbed on SWCNT. It was difficult to estimate the number of Pcs per SWCNT using the reported procedures [36] because the SWCNT did not decompose completely.

Table 2. Thermogravimetric analysis (TGA) data of complexes 1-3.

Temperature (°C)	ZnTPCPc-uridine-SWCNT (% weight loss)	SWCNT-COOH (% weight loss)	ZnTPCPc-uridine (% weight loss)
26	100	100	100
50	98.9	98.9	99.9
80	95.5	95.3	99.2
100	94.2	91.8	98.5
150	92.8	86.4	91.5
180	92.2	85.1	83.5
200	91.8	84.4	75.6
250	90.8	81.5	60.8
300	89.6	76.9	53.4
350	87.1	72.9	48.9
400	83.4	67.0	41.5
450	74.6	57.1	32.4
500	64.1	42.6	28.5

3.3 Raman Spectroscopy

Raman spectroscopy is used to determine the functionalization of a material. Complex 3 showed prominent peaks at 1261, 1587, and 2500 cm^{-1} wavenumber; these peaks were also observed in SWCNTs at low intensity. Research has shown that SWCNTs exhibit signature Raman peaks (Fig.4) at about 2500 cm^{-1} (G*), 1590 cm^{-1} (G-band (tangential mode); sp^2)) [36, 37] and 1270 cm^{-1} (D (disorder band, (breathing mode); sp^3). The changes observed in the intensity of the peaks point to the differences in the morphology of SWCNTs after the adsorption of ZnTPCPc-uridine. The D: G ratio is a parameter for determining the functionalization extent of carbon nanotubes. The D band intensity is usually higher on functionalization [38-39], increasing D: G ratio. There is a difference in the D: G ratio of SWCNTs after modification with ZnTPCPc-uridine to form ZnTPCPc-uridine-SWCNT. Increases in the G band are

also associated with the removal of some amorphous carbon from the nanotubes [40].
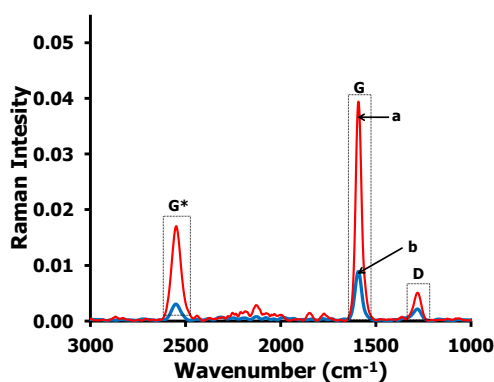
Fig. 4. Raman spectra of (a) ZnTPCPc-uridine-SWCNT, (3); and (b) SWCNT-COOH. G* is the non-dispersive phonon mode, G is the tangential vibrational mode (sp^2) and D is the breathing mode; disorder band (sp^3).

3.4 Transmission electron microscopy (TEM)

Transmission electron microscopy was used to further characterize complex 3 as shown in Fig. 5. The TEM image shows that there is a strong interaction between ZnTPCPc-uridine and SWCNT after adsorption. The image of ZnTPCPc-uridine-SWCNT and SWCNT-COOH are quite different suggesting the successful formation of complex 3. Fig. 5 shows an average size of about 4-15 nm in diameter for the nanotubes. Different sizes are observed due to SWCNTs overlapping with each other, which could be a result of aggregation.
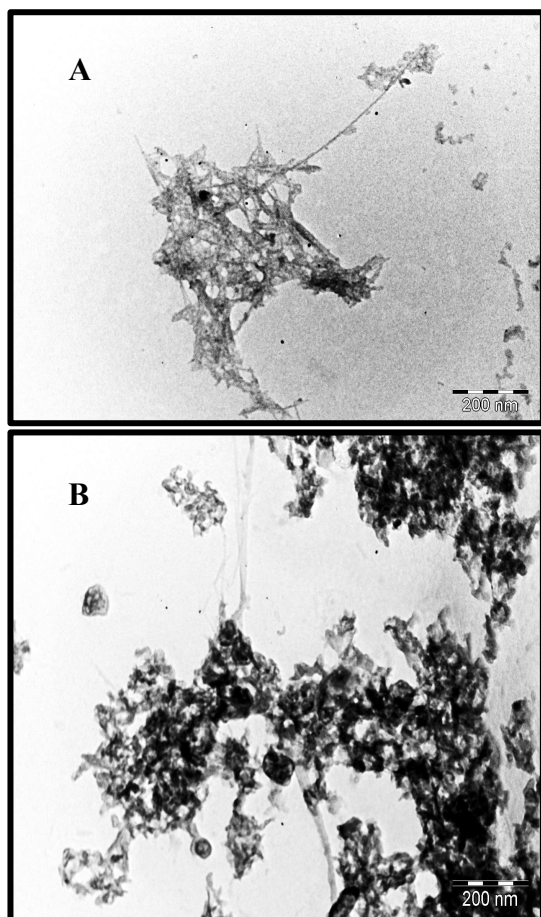
Fig. 5. TEM Image of SWCNT-COOH (A) ZnTPCPc-uridine-SWCNT 6 (B).

3.5 Photophysical properties

3.5.1 Fluorescence Quantum (Φ_F) yield

The fluorescence quantum yields (Φ_F) were calculated for complexes 1, 2, and 3 on excitation at 610 nm at an absorbance of 0.05. The Φ_F of complex ZnTPCPc (1), ZnTPCPc-uridine (2), and ZnTPCPc-uridine-SWCNT (3) are 0.1, 0.13, and 0.16, respectively. There was a slight increase in the Φ_F complexes 2 and 3. The intrinsic fluorescence property of uridine [41] is responsible for the slight increase in the Φ_F of the ZnTPCPc in the presence of uridine.

3.5.2 Triplet quantum yield (Φ_T)

The triplet quantum yield of 1, 2, and 3 is given as 0.49, 0.56, and 0.78, respectively. The presence of spacers such as phenyl links has been reported to support the spin-orbit charge transfer intersystem crossing (SOCT-ISC) mechanism, which results in a fast intersystem crossing rate from excited singlet state to triplet state [42]. The phenoxyl carboxy group is a typical example of a linker between ZnTPCPc and uridine moiety; this may be responsible for the high triplet quantum yield exhibited by complexes 2 and 3. The increase in triplet quantum yield for 3 is surprising; SWCNTs, an electron-accepting group, are known to quench photoexcited complexes such as electron-donating phthalocyanine, thereby impacting the triplet quantum yield [43, 44]. The increase in triplet quantum yield (Φ_T) of complex 3 may be due to the formation of radical pairs by the two complexes which have been shown to support radical-pair intersystem crossing (RP-ISC) [43-46].

4. Conclusion

The synthesis of zinc tetra phenoxy carboxy phthalocyanine (ZnTPCPc)- uridine and ZnTPCPc-uridine-SWCNT is reported for the first time. The conjugates were synthesized and characterized by different spectroscopic

methods which include FTIR, UV, and mass spectrometer. The results showed the successful formation of the complexes. ZnTPCPc-uridine-SWCNT (3) is more thermally stable when compared to ZnTPCPc or SWCNT alone. The fluorescence and triplet quantum yield of complex 3 increases in the presence of SWCNT (over 20 %) despite the known quenching effects of SWCNT. This suggests that the new combined photoactive complex could be a potential drug for the treatment of cancer.

References

[1] Iijima S. Helical microtubules of graphitic carbon. Nature, 1991;354,56-8.

[2] Teradal NL, Jelinek R. Carbon Nanomaterials in biological studies and biomedicine. Adv Healthc Mater 2017;6:2192-640.

[3] Tang L, Xiao Q, Mei Y, He S, Zhang Z, Wang R, Wang W. Insights on functionalized carbon nanotubes for cancer theranostics. J Nanobiotechnol 2021;19,423-51.

[4] Chaudhuri P, Soni S, Sengupta S. Single-walled carbon nanotube-conjugated chemotherapy exhibits increased therapeutic index in melanoma. Nanotechnology 2010; 21:25102-11.

[5] Dubey R, Dutta D, Sarkar A, Chattopadhyay P. Functionalized carbon nanotubes: synthesis, properties and applications in water purification, drug delivery, and material and biomedical sciences. Nanoscale Adv., 2021;3,5722-44.

[6] Kam NWS, O'Connell M, Wisdom JA, Dai H. Carbon nanotubes as multifunctional biological transporters and near-infrared agents for selective cancer cell destruction. Proc. Natl. Acad. Sci. 2005;102:11600-5.

[7] Algorri JF, Ochoa M, Roldán-Varona P, Rodríguez-Cobo L, López-Higuera, JM. Photodynamic Therapy: A Compendium of Latest Reviews. Cancers (Basel). 2021;17:4447.

[8] Zimcik P, Miletin M, Ponec J, Kostka M, Fiedler Z. Synthesis and studies on photodynamic activity of new water-soluble azaphthalocyanines. J. Photochem, Photobiol., A, 2003; 155:127-31.

[9] Niculescu AG, Grumezescu A, Photodynamic Therapy-An Up-to-Date Review. Appl. Sci. 2021;11:3626.

[10] Ogbodu RO, Antunes E, Nyokong T. Physicochemical properties of zinc monoamino phthalocyanine conjugated to folic acid and single walled carbon nanotubes. Polyhedron, 2013;60:59-67.

[11] Kenny ME, Liu Y. Photodynamic Therapy with Phthalocyanine and Radical Sources. US 2012/0323164 A1.

[12] Ogbodu RO, Leigh J, Prinsloo EA, Nyokong T. Photophysical properties and photodynamic effect of zinc phthalocyanine-spermine-single-walled carbon nanotube conjugate against MCF-7 breast cancer cell line. Synthetic Metals 2015;204:122-32.

[13] Khoza P, Antunes E, Chen JY, Nyokong T. Khoza P, Antunes E, Chen J-Y, Nyokong T. Synthesis and photophysicochemical studies of a water soluble conjugate between folic acid and zinc tetraaminophthalocyanine. J Lumin 2013;134:784-90.

[14] Haakensen VD, Biong M, Lingjærde OC, Holmen MM, Frantzen JO, Chen Y, Navjord D, et.al., Expression levels of uridine 5'-diphospho-glucuronosyltrans-

ferase genes in breast tissue from healthy women are associated with mammographic density. Breast Cancer Res 2010;12:1-11.

[15] Grove KL, Chene YC. Uptake and Metabolism of the New Anticancer Compound β-l-(-)-Dioxolane-Cytidine in Human Prostate Carcinoma DU-145 Cells. Cancer Res1996;56:4187-91.

[16] Nagar S, Remmel RP. Uridine diphosphoglucuronosyltransferase pharmacogenetics and cancer. Oncogene, 2006;25:1659-72.

[17] Guillemette C, Millikan RC, Newman B, Housman DE. Genetic polymorphisms in uridine diphospho-glucuronosyltransferase 1A1 and association with breast cancer among African Americans. Cancer Res 2000;60:950-6.

[18] Shen XM, Zheng BY, Huang XR, Wang L, Huang JD. The first silicon (IV) phthalocyanine--nucleoside conjugates with high photodynamic activity. Dalton Trans 2013;42:10398-403.

[19] Hampel S1, Kunze D, Haase D, Krämer K, Rauschenbach M, Ritschel M, Leonhardt A, Thomas J, Oswald S, Hoffmann V, Büchner B. Carbon nanotubes filled with a chemotherapeutic agent: a nanocarrier mediates inhibition of tumor cell growth. Int J Nanomed 2008;3:175-82.

[20] Borzęcka W, Domiński A, Kowalczuk M. Recent Progress in Phthalocyanine-Polymeric Nanoparticle Delivery Systems for Cancer Photodynamic Therapy. Nanomaterials. 2021;11:2426.

[21] Bianco A, Kostarelos K, Partidos CD, Prato M. Biomedical applications of functionalised carbon nanotubes. Chem Commun 2005;5:571-7.

[22] Nazeeruddin MDK, Humphry-Baker R, Grätzel M, Wöhrle D, Schnurpfeil G, Schneider G, Hirth A, Trombach N. Efficient near-IR sensitization of nanocrystalline TiO 2 films by zinc and aluminum phthalocyanines. J Porphyrins Phthalocyanines 1999;3:230-7.

[23] D'Souza S, Antunes E, Litwinski C, Nyokong T. Photophysical behavior of zinc monoaminophthalocyanines linked to mercaptopropionic acid-capped CdTe quantum dots. J Photochem Photobiol A 2011;220:11-9.

[24] Masilela N, Nyokong T. Conjugates of low-symmetry Ge, Sn and Ti carboxy phthalocyanines with glutathione caped gold nanoparticles: an investigation of photophysical behavior. J Photochem Photobiol A 2011;223:124-31.

[25] Fashina A, Antunes E, Nyokong T. Silicananoparticles grafted with phthalocyanines: photophysical properties and studies in artificial lysosomal fluid. New J Chem 2013;37: 2800-9.

[26] Nakashima N, Tomonari Y, Murakami H. Water-soluble single-walled carbon nanotubes via noncovalent sidewall-functionalization with a pyrene-carrying ammonium ion. Chem Lett 2002;31:638-9.

[27] Tran-Thi TH, Desforge C, Thiec C, Singlet-singlet and triplet-triplet intramolecular transfer processes in a covalently linked porphyrin-phthalocyanine heterodimer. J Phys Chem 1989;93:1226-33.

[28] Kubat P, Mosinger J. Photophysical properties of metal complexes of meso-tetrakis (4-sulphonatophenyl) porphyrin. J Photochem. Photobiol A 1996;96:93-7.

[29] Frey-Forgues S, Lavabre D, Are Fluorescence Quantum Yields So Tricky to Measure? A Demonstration Using Familiar Stationery Products. J Chemic Educ 1999;76:1260.

[30] Ogunsipe A, Maree D, Nyokong T. Solvent effects on the photochemical and fluorescence properties of zinc phthalocyanine derivatives. J Mol Struct 2003;650:131-40.

[31] Kabay N, Baygu Y, Ak M, Kara İ, Kaya E, Durmuş M, Gök Y. Novel nonperipheral octa-3-hydroxypropylthio substituted metallo-phthalocyanines: synthesis, characterization, and investigation of their electrochemical, photochemical and computational properties. Turk J Chem. 2021;45:143-56.

[32] Pişkin M, Odaba Z. Synthesis, Characterization and Spectroscopic Properties of Novel Mono-Lutetium(Iıı) Phthalocyanines. Karaelmas Fen ve Müh. Derg. 2016;6:307-14.

[33] Wang X, Liu Y, Qiu W, Zhu D,. Immobilization of tetra-tert-butylphthalocyanines on carbon nanotubes: a first step towards the development of new nanomaterials. J. Mater. Chem. 2002;12: 1636-9.

[34] Ballesteros B, Campidelli S, Torre G, Ehli C, Guldi DM, Prato M, Torres T. Synthesis, characterization and photophysical properties of a SWNT-phthalocyanine hybrid. Chem. Commun. 2007;28:2950-2.

[35] Jiang BP, Hu LF, Wang DJ, Ji SC, Shen XC, Liang H. Graphene loading water-soluble phthalocyanine for dual-modality photothermal/photodynamic therapy via a one-step method. Journal of Materials Chemistry B. 2014;2(41):7141-8.

[36] Ballesteros B, Torre G, Ehli C, Aminur Rahman GM, Agullo-Rueda F, Guldi DM, Torres T. Single-wall carbon nanotubes bearing covalently linked phthalocyanines-photoinduced electron transfer. J Am Chem Soc 2007;129:5061-8.

[37] Dresselhaus MS, Dresselhaus G, Jorio A. Raman spectroscopy of carbon nanotubes in 1997 and 2007. J Phys Chem C 2007;111:17887-93.

[38] Chidawanyika W, Nyokong T. Characterization of amine-functionalized single-walled carbon nanotube-low symmetry phthalocyanine conjugates. Carbon, 2010;48:2831-8.

[39] Dillon EP, Crouse CA, Barron AR. Synthesis, Characterization, and Carbon Dioxide Adsorption of Covalently Attached Polyethyleneimine-Functionalized Single-Wall Carbon Nanotubes. Nano 2008;2:156-64.

[40] Yang K, Gu M, Guo Y, Pan X, Mu G. Effects of carbon nanotube functionalization on the mechanical and thermal properties of epoxy composites. Carbon, 2009;47:1723-37.

[41] Li J, Fang X, Ming X. Visibly Emitting Thiazolyl-Uridine Analogues as Promising Fluorescent Probes. The Journal of Organic Chemistry. 2020;85(7):4602-10.

[42] Colvin MT, Ricks AB, Scott AM, Co DT, Wasielewski MR. Intersystem crossing involving strongly spin exchange-coupled radical ion pairs in donor-bridge-acceptor molecules. J Phys Chem A 2012;116:1923-30.

[43] Bottari G, Torre G, Guldi DM, Torres T. Covalent and noncovalent-phthalocyananine-carbon nanostructure

systems: synthesis photonduced electron transfer, and application to molecular photovoltaics. Chem Rev 2010;110:6768-816.

[44] Bottari G, Suanzes JA, Trukhina O, Torres T. Phthalocyanine-carbon nanostructure materials assembled through supramolecular interactions. J Phys Chem Lett 2011;2: 905-13.

[45] Avalos CE, Richert S, Socie E, Karthikeyan G, Casano G, Stevanato G, Kubicki DJ, Moser JE, Timmel CR, Lelli M, Rossini AJ. Enhanced intersystem crossing and transient electron spin polarization in a photoexcited pentacene–trityl radical. The Journal of Physical Chemistry A. 2020;124(29):6068-75.

[46] Sarfraz A, Raza AH, Mirzaeian M, Abbas Q, Raza R. Electrode Materials for Fuel Cells. Encyclopedia of Smart Materials, 2022;2:341-56.